

# Effect of symmetries in out-of-time ordered correlators in interacting integrable and nonintegrable many-body quantum systems

Vinitha Balachandran,<sup>1</sup> Lea F. Santos,<sup>2</sup> Marcos Rigol,<sup>3</sup> and Dario Poletti<sup>1, 4, 5, 6</sup>

<sup>1</sup>*Science, Mathematics and Technology Cluster, Singapore University of Technology and Design, 8 Somapah Road, 487372 Singapore*

<sup>2</sup>*Department of Physics, University of Connecticut, Storrs, Connecticut 06269, USA*

<sup>3</sup>*Department of Physics, The Pennsylvania State University, University Park, PA 16802, USA*

<sup>4</sup>*EPD Pillar, Singapore University of Technology and Design, 8 Somapah Road, 487372 Singapore*

<sup>5</sup>*The Abdus Salam International Centre for Theoretical Physics, Strada Costiera 11, 34151 Trieste, Italy*

<sup>6</sup>*Centre for Quantum Technologies, National University of Singapore 117543, Singapore*

Out-of-time ordered correlators (OTOCs) help characterize the scrambling of quantum information and are usually studied in the context of nonintegrable systems. We compare the relaxation dynamics of OTOCs in interacting integrable and nonintegrable many-body quantum systems in the presence of  $U(1)$  symmetry and supersymmetry. We show that their dynamics exhibit similar behaviors, with a time dependence that is mostly determined by the symmetry rather than integrability, and they follow closely the dynamics of two-point correlators. We study the OTOCs dynamics using numerical calculations, and gain analytical insights from the properties of the diagonal and of the off-diagonal matrix elements of the OTOCs local operators in the energy eigenbasis.

## I. INTRODUCTION

Out-of-time-ordered correlators (OTOCs) are a diagnostic of quantum information scrambling [1–14] and can be measured experimentally [15–23]. In quantum systems with a classical limit, OTOCs grow exponentially fast as a result of chaos [24–36] or of instabilities in integrable systems [37–42]. Due to the relationship with chaos in classical systems, connections between the behavior of OTOCs and the onset of thermalization have been discussed [3–13]. In nonintegrable models with local conserved quantities, OTOCs have been shown to exhibit a slower (algebraic) growth when the operators involved have an overlap with a conserved quantity [43–48]. This behavior has been explained in terms of the Lieb-Robinson bounds [49, 50] and of the eigenstate thermalization hypothesis (ETH) [48]. In this work, we explore the effects of symmetries, such as  $U(1)$  and supersymmetry, in the OTOCs dynamics of interacting integrable and nonintegrable many-body quantum systems.

Interacting integrable systems have been extensively studied theoretically in recent years because of their relevance to experiments [51, 52], and this has resulted in remarkable progress in understanding their dynamics [53]. In those systems, after reaching equilibrium following unitary dynamics, observables are not described by traditional Gibbs ensembles [54–56], but by generalized Gibbs ensembles that incorporate all the conserved quantities that make the models integrable [57–59]. Furthermore, as a result of the presence of an extensive number of conservation laws, the large-distance dynamics of integrable models is different from regular hydrodynamics [60–62], and it is described by a generalized hydrodynamics [63, 64].

We compare the evolution of OTOCs in an integrable and a nonintegrable spin-1/2 XYZ chain. Our numerical results and analytical insights elucidate the role of sym-

metries and their associated local conservation laws. We first highlight that, in the presence of symmetries, the OTOCs can mirror the behavior of two-time correlators for long times. We then show that, within the system sizes and timescales that we consider, the OTOCs dynamics for both interacting integrable and nonintegrable many-body quantum systems can be qualitatively and quantitatively analogous. The OTOCs for interacting integrable and nonintegrable models can exhibit an algebraic decay in the presence of symmetries, and a faster (exponential-like) relaxation in their absence. Analytical insights are obtained using the relation between the dynamics of the OTOCs and the behavior of the matrix elements of the operators involved in the OTOCs in the energy eigenbasis; specifically, the behavior of the diagonal matrix elements in finite systems, and the behavior of the off-diagonal elements in the thermodynamic limit.

The presentation is organized as follows. In Sec. II, we use the properties of the matrix elements of the OTOCs operators written in the eigenenergy basis to provide a general understanding of the OTOCs relaxation dynamics. Our analytical insights are tested using numerical simulations of the spin-1/2 XYZ model in Sec. III. A summary of our results is provided in Sec. IV.

## II. OTOC DECAY AND MATRIX ELEMENTS OF LOCAL OPERATORS

For operators  $\hat{A}$  and  $\hat{B}$ , the infinite-temperature OTOC is defined as

$$O^{AB}(t) = \langle [\hat{A}(t), \hat{B}][\hat{A}(t), \hat{B}]^\dagger \rangle / 2, \quad (1)$$

where  $\hat{A}(t) = \hat{U}^\dagger(t)\hat{A}\hat{U}(t)$  is the time-evolved operator  $\hat{A}$  under the unitary evolution operator  $\hat{U}(t) = \mathcal{T}e^{-i\int_0^t \hat{H}(\tau)d\tau}$ , with  $\mathcal{T}$  indicating the time-ordered integration, and  $\hat{H}(t)$  being a general time-dependent Hamil-

tonian. By infinite-temperature OTOC we mean that  $\langle \dots \rangle = \text{tr}(\dots)/\mathcal{V}$ , where  $\mathcal{V}$  is the relevant Hilbert space dimension. Equation (1) can be rewritten as

$$O^{AB}(t) = G^{AB}(t) - F^{AB}(t), \quad (2)$$

where

$$G^{AB}(t) = \langle \hat{B} \hat{A}(t) \hat{A}(t)^\dagger \hat{B}^\dagger \rangle \quad (3)$$

equals 1 for unitary operators, which are the focus of this work, and

$$F^{AB}(t) = \langle \hat{A}(t) \hat{B} \hat{A}(t) \hat{B} \rangle. \quad (4)$$

In what follows, we study the time evolution of  $F^{AB}(t)$ .

For a time-independent Hamiltonian with eigenenergies  $E_\alpha$  and eigenkets  $|\alpha\rangle$ , Eq. (4) can be written as

$$F^{AB}(t) = \frac{1}{\mathcal{V}} \sum_{\alpha, \beta, \gamma, \delta} e^{i(E_\alpha - E_\beta + E_\gamma - E_\delta)t} A_{\alpha\beta} B_{\beta\gamma} A_{\gamma\delta} B_{\delta\alpha}, \quad (5)$$

where  $A_{\alpha\beta} = \langle \alpha | \hat{A} | \beta \rangle$ ,  $B_{\beta\gamma} = \langle \beta | \hat{B} | \gamma \rangle$ . We work in units in which  $\hbar = 1$ .

Next, we discuss two ways in which one can gain an analytic understanding of the OTOCs decay. The first one involves infinite-time averages in finite systems, and the second one involves the structure of the off-diagonal matrix elements of the operators of interest in the energy eigenbasis in the thermodynamic limit. Our focus is on traceless operators  $\hat{A}$  and  $\hat{B}$  that, in addition to being unitary, are local and Hermitian (i.e., that can correspond to physical observables).

### A. OTOC decay and infinite-time averages

Under the assumption of unequal energy spacings,

$$E_\alpha - E_\beta = E_\gamma - E_\delta \implies \begin{cases} E_\alpha = E_\beta \text{ and } E_\gamma = E_\delta \\ \text{or} \\ E_\alpha = E_\delta \text{ and } E_\beta = E_\gamma, \end{cases} \quad (6)$$

one finds that the infinite-time average of Eq. (5) (describing the long-time results) is

$$F^{AB}(\infty) = \frac{1}{\mathcal{V}} \left[ \sum_{\alpha} A_{\alpha\alpha}^2 B_{\alpha\alpha}^2 \right. \quad (7) \\ \left. + \sum_{\beta, \alpha \neq \beta} (A_{\beta\beta} A_{\alpha\alpha} |B_{\beta\alpha}|^2 + |A_{\beta\alpha}|^2 B_{\beta\beta} B_{\alpha\alpha}) \right].$$

Assumption (6) for the eigenenergies is traditionally expected to hold for nonintegrable quantum systems [65], and Eq. (7) has been recently verified to be a good approximation for numerical results of OTOCs in such systems [48, 66]. Assumption (6) is also expected to hold

for interacting integrable quantum systems, which have a Poisson-like level spacing distribution, i.e., the eigenenergies behave as uncorrelated random numbers and, consequently, do not exhibit equal energy spacings or a large number of degeneracies like the ones found in noninteracting models [67]. Here, we show that Eq. (7) can also be used in the context of interacting integrable quantum systems.

Equation (7) can be further simplified under the assumption that the eigenstate to eigenstate fluctuations of  $A_{\alpha\alpha}$  and  $B_{\alpha\alpha}$ , for *all* eigenstates with the same energy density, vanish in the thermodynamic limit at least polynomially with the system size [66]. Under this assumption, if operator  $\hat{A}$  or  $\hat{B}$  has a nonzero overlap with the local Hamiltonian, then the diagonal matrix elements of the operator decay algebraically with the system size. Since we are considering unitary operators, this implies that the first sum in the r.h.s. of Eq. (7) decays to zero, as a function of the system size, faster than the second sum. Hence, the results in Ref. [66] allow us to simplify Eq. (7) to

$$F^{AB}(\infty) \approx \frac{1}{\mathcal{V}} \sum_n (A_{\alpha\alpha}^2 + B_{\alpha\alpha}^2). \quad (8)$$

One can then see that  $F^{AB}(\infty)$  is nonzero whenever the diagonal matrix elements of  $\hat{A}$  or  $\hat{B}$  are nonzero.

The assumption that the eigenstate to eigenstate fluctuations of  $A_{\alpha\alpha}$  and  $B_{\alpha\alpha}$ , for *all* eigenstates with the same energy density, vanishes in the thermodynamic limit has been found to hold for physical observables (represented by few-body operators) in nonintegrable systems [68], with a decrease of the fluctuations that is exponential with the system size [69–71], as opposed to the weaker polynomial decrease required in Ref. [66]. This assumption is violated in integrable systems, but only by a vanishing fraction of the eigenstates with the same energy density. In integrable systems, the variance of the diagonal matrix elements has been found to decay as a power law with the system size [72–76]. This helps understanding why, as we will show, Eq. (8) can also be used to gain insights into the behavior of OTOCs in interacting integrable systems.

If one invokes the Lieb-Robinson bound, which bounds the speed of the propagation of correlations in local and bounded Hamiltonians [77, 78], one can use Eqs. (7)–(8) in finite systems to predict what happens in the thermodynamic limit at finite times. Because of the bound, an accurate description of the evolution of the OTOCs in the thermodynamic limit can be obtained by considering a finite system of size  $L_{\text{LR}}$ ,

$$F_{L=\infty}^{AB}(t) \approx F_{L_{\text{LR}}}^{AB}(t), \quad (9)$$

where  $L_{\text{LR}} \equiv s v_{\text{LR}} t$ ,  $v_{\text{LR}}$  is the Lieb-Robinson velocity  $v_{\text{LR}}$ , and  $s$  is a real number larger than 1.

Assuming that the system is maximally scrambled within the region of size  $L_{\text{LR}}$ , one can write

$$F_{L=\infty}^{AB}(t) \approx F_{L_{\text{LR}}}^{AB}(\infty), \quad (10)$$

which, since  $L_{\text{LR}}$  increases with time, is a time-dependent quantity. If  $F_L^{AB}(\infty)$  decays algebraically with the system size, *i.e.*, if

$$F_L^{AB}(\infty) \propto \frac{1}{L^\eta}, \quad (11)$$

which, as mentioned before, occurs if the operator  $\hat{A}$  or  $\hat{B}$  has a nonzero overlap with the local Hamiltonian [66], then the OTOC in the thermodynamic limit decays algebraically in time

$$F_{L=\infty}^{AB}(t) \propto \frac{1}{t^\eta}. \quad (12)$$

If the system is not maximally scrambled as assumed before, then the decay of  $F_{L=\infty}^{AB}(t)$  is slower, *i.e.*,  $F_{L_{\text{LR}}}^{AB}(\infty)$  is a lower bound for the relaxation dynamics of  $F_{L=\infty}^{AB}(t)$ . Slower dynamics than the one predicted by this bound occurs, for example, in systems that undergo prethermalization [79, 80]. On the other hand, if the diagonal matrix elements of the traceless operators  $\hat{A}$  and  $\hat{B}$  are already vanishingly small in finite systems, the infinite-time average  $F_L^{AB}(\infty) \approx 0$ , and the decay of  $F_{L=\infty}^{AB}(t)$  can be faster than algebraic, *e.g.*, exponential [43, 48]. A comprehensive analysis of these features for nonintegrable systems can be found in Ref. [48].

We stress that, as we will show using numerical calculations in the following sections, the results in this section can be invoked in the context of both interacting integrable and nonintegrable many-body systems. Both classes of systems exhibit “generic spectra” in the sense of Eq. (6) and a vanishing fraction of eigenstates that do not exhibit eigenstate thermalization for (few-body) operators representing physical observables.

## B. OTOC decay and two-time correlators

One can also gain an understanding of the decay of the OTOCs in interacting integrable and nonintegrable many-body systems using the properties of the off-diagonal matrix elements of local operators in the energy eigenstates. To do this, we note that Eq. (8) corresponds to the infinite-time average of the two-time correlator

$$C^{AB}(t) = \langle \hat{A}(t)\hat{A}(0) \rangle + \langle \hat{B}(t)\hat{B}(0) \rangle. \quad (13)$$

Within the Lieb-Robinson argument discussed earlier in the context of Eqs. (9)–(12), this implies that the slow dynamics of the OTOCs is a result of the slow dynamics of the two-time correlator  $\langle \hat{A}(t)\hat{A}(0) \rangle$  or  $\langle \hat{B}(t)\hat{B}(0) \rangle$ . The OTOCs can decay fast in time only if both two-time correlators decay fast in time.

Let us then analyze the dynamics at long times of a two-time correlator, say of operator  $\hat{A}$ , to see how it is related to the structure of its off-diagonal elements in the eigenenergy basis. In nonintegrable systems, one can use that, according to the ETH, the matrix elements of

local operators in the energy eigenbasis can be written as [68, 81–83]

$$A_{\alpha\beta} = A(\bar{E}_{\alpha\beta})\delta_{\alpha\beta} + e^{-S(\bar{E}_{\alpha\beta})/2}f^A(\bar{E}_{\alpha\beta}, \omega_{\alpha\beta})R_{\alpha\beta}, \quad (14)$$

where  $\bar{E}_{\alpha\beta} = (E_\alpha + E_\beta)/2$ ,  $\omega_{\alpha\beta} = E_\alpha - E_\beta$ ,  $S(\bar{E})$  is the thermodynamic entropy at energy  $\bar{E}$ , the functions  $A(\bar{E}_{\alpha\beta})$  and  $f^A(\bar{E}_{\alpha\beta}, \omega_{\alpha\beta})$  are smooth functions of their arguments, and  $R_{\alpha\beta}$  are random numbers with zero mean and unit variance. For bounded lattice Hamiltonians like the ones of interest here, the overwhelming majority of the eigenstates is at “infinite temperature”, *i.e.*, the extensive part of their eigenenergies is  $E_\infty \equiv \text{tr}(\hat{H})/\mathcal{V}$ . When  $\bar{E}_{\alpha\beta} = E_\infty$ ,  $\exp[-S(E_\infty)] \simeq 1/\mathcal{V}$ , and the ETH ansatz simplifies to

$$A_{\alpha\beta} \simeq A(E_\infty)\delta_{\alpha\beta} + \frac{1}{\sqrt{\mathcal{V}}}f^A(E_\infty, \omega_{\alpha\beta})R_{\alpha\beta}. \quad (15)$$

With that in mind, one can write the two-time correlator for the operator  $\hat{A}$  as

$$\langle A(t)A(0) \rangle \simeq \frac{1}{\mathcal{V}^2} \sum_{\alpha, \beta} e^{i\omega_{\alpha\beta}t} |R_{\alpha\beta}|^2 |f^A(E_\infty, \omega_{\alpha\beta})|^2. \quad (16)$$

Since the  $f^A$  functions decay rapidly with increasing frequency [68], one can replace the sums by integrals using that the density of states at infinite temperature is  $\simeq \mathcal{V}$ , and we find

$$\langle A(t)A(0) \rangle \simeq \int d\omega \cos(\omega t) |f^A(E_\infty, \omega)|^2. \quad (17)$$

Hence, the low-frequency behavior of  $|f^A(E_\infty, \omega)|^2$  (or  $|f^B(E_\infty, \omega)|^2$ ) determines the relaxation dynamics of the OTOCs. Specifically, structure (nonzero  $\omega$  derivative) at low frequency results in a slow decay of the OTOCs while lack of structure (*e.g.*, a plateau) results in a fast (exponential-like) decay of the OTOCs.

It has been recently shown that, like in nonintegrable many-body quantum systems, the vanishing off-diagonal matrix elements of local operators in the energy eigenstates of interacting integrable many-body quantum systems are measure zero of all the matrix elements, *i.e.*, the off-diagonal matrix elements are dense [71]. This is to be contrasted to what happens in noninteracting systems, in which the vanishing matrix elements are measure one, *i.e.*, the off-diagonal matrix elements are sparse [76]. Hence, in interacting integrable many-body quantum systems one can define a meaningful function that parallels  $|f^{A/B}(\bar{E}, \omega)|^2$  in Eq. (14). At  $\bar{E} = E_\infty$ , such a function has been shown to be a smooth function of  $\omega$  for various local observables [71, 84–86]. Hence, we expect that the analysis leading to Eq. (17) holds for interacting integrable systems and, with it, the analytic insights that the equation provides. We should add that an important difference between the behavior of the off-diagonal

matrix elements of nonintegrable and interacting integrable systems, which does not change our analysis here, is that in the former the  $R_{\alpha\beta}$  random numbers are normally distributed while in the latter they are not [71]. For integrable systems it was recently shown that the distributions are well described by generalized Gamma distributions [76].

### III. NUMERICAL RESULTS

We consider the spin-1/2 XYZ model described by the following Hamiltonian,

$$\begin{aligned} \hat{H} &= \hat{H}_I + \hat{H}_{NI}, \\ \hat{H}_I &= \sum_{l=1}^{L-1} [J^x \hat{\sigma}_l^x \hat{\sigma}_{l+1}^x + J^y \hat{\sigma}_l^y \hat{\sigma}_{l+1}^y + J^z \hat{\sigma}_l^z \hat{\sigma}_{l+1}^z], \\ \hat{H}_{NI} &= \Lambda \sum_{l=1}^{L-1} (-1)^l \hat{\sigma}_l^z \hat{\sigma}_{l+1}^z. \end{aligned} \quad (18)$$

where  $J^a$  are the coupling strengths along the  $a = x, y$ , and  $z$  directions,  $\hat{\sigma}_l^a$  is represented by the  $a$  Pauli matrix for site  $l$ , and  $L$  is the number of lattice sites.  $\hat{H}_I$  is an interacting integrable Hamiltonian that can be solved analytically using the eight vertex model [87, 88]. The addition of the staggered interactions,  $\hat{H}_{NI}$ , of magnitude  $\Lambda$  along the  $z$ -direction, breaks integrability.

The symmetries of the total Hamiltonian  $\hat{H}$  are:

(i) The parity operators along each axis,  $\hat{P}^a = \prod_l \hat{\sigma}_l^a$ , commute with the total Hamiltonian. (ia) When  $L$  is even, the parity operators also commute with each other. As a result, the diagonal matrix elements of the local operators  $\hat{\sigma}_l^a$  in the energy eigenstates are exactly zero (numerically, we find them to be of the order of  $10^{-14}$ ), unless there are other symmetries such as those discussed next in (ii) and (iii). We can understand this as follows, for  $L$  even, the energy eigenkets  $|\alpha\rangle$  (where  $\hat{H}|\alpha\rangle = E_\alpha|\alpha\rangle$ ) are simultaneous eigenkets of the three operators  $\hat{P}^a$ . Hence, we can write

$$\langle \alpha | \hat{\sigma}_l^z | \alpha \rangle = \langle \alpha | \hat{P}^x \left( \hat{P}^x \hat{\sigma}_l^z \hat{P}^x \right) \hat{P}^x | \alpha \rangle = -\langle \alpha | \hat{\sigma}_l^z | \alpha \rangle = 0, \quad (19)$$

where we used that  $\hat{P}^x \hat{\sigma}_l^z \hat{P}^x = -\hat{\sigma}_l^z$  and that  $\hat{P}^x | \alpha \rangle = \pm | \alpha \rangle$ . (ib) When the system size  $L$  is odd, the parity operators anticommute with each other. As a result, one finds that the diagonal matrix elements of the local operators  $\hat{\sigma}_l^a$  in the energy eigenstates need not vanish, which is what we observe numerically. We can understand this as follows, for  $L$  odd, the energy eigenkets  $|\alpha\rangle$  are not simultaneous eigenkets of the three operators  $\hat{P}^a$ . Let us choose the energy eigenkets to be simultaneous eigenkets of  $\hat{P}^z$ . If  $|\alpha_+\rangle$  is an energy eigenket with eigenenergy  $E_\alpha$  satisfying  $\hat{P}^z |\alpha_+\rangle = |\alpha_+\rangle$ , then  $\hat{P}^x |\alpha_+\rangle = |\alpha_-\rangle$  is an energy eigenket with eigenenergy  $E_\alpha$  (because  $\hat{P}^x$  and  $\hat{H}$

commute) satisfying  $\hat{P}^z |\alpha_-\rangle = -|\alpha_-\rangle$  (because  $\hat{P}^x$  and  $\hat{P}^z$  anticommute), i.e., the energy spectrum is doubly degenerate [89]. For the diagonal matrix elements of the local operators, instead of Eq. (19) we have

$$\begin{aligned} \langle \alpha_+ | \hat{\sigma}_l^z | \alpha_+ \rangle &= \langle \alpha_+ | \hat{P}^x \left( \hat{P}^x \hat{\sigma}_l^z \hat{P}^x \right) \hat{P}^x | \alpha_+ \rangle \\ &= -\langle \alpha_- | \hat{\sigma}_l^z | \alpha_- \rangle, \end{aligned} \quad (20)$$

i.e., they need not vanish. With increasing system size, one expects that the difference between the results obtained for chains with  $L$  and  $L+1$  sites decreases, and vanish in the thermodynamic limit. Our numerical results are consistent with that expectation.

(ii) In general, the integrable Hamiltonian  $\hat{H}_I$  does not conserve total magnetization in any direction, except when two of the coupling parameters are equal, in which case the model exhibits a  $U(1)$  symmetry and reduces to the spin-1/2 XXZ chain (upon relabeling, if needed,  $x$ ,  $y$ , and  $z$  so that  $J_z \neq J_x = J_y$ ). For  $\Lambda \neq 0$ , the  $U(1)$  symmetry is only present for  $\hat{H}$  if  $J_x = J_y$ .

One can show that if  $\hat{H}$  has  $U(1)$  symmetry, i.e., if  $\hat{S}^z = \sum_l \hat{\sigma}_l^z$  is conserved, then the diagonal matrix elements of the local operators  $\hat{\sigma}_l^z$  in the energy eigenstates need not vanish. Considering  $L$  even, we have already mentioned that  $\hat{P}^x$ ,  $\hat{P}^y$ , and  $\hat{P}^z$  commute with each other and with the Hamiltonian. However, only  $\hat{P}^z$  commutes with  $\hat{S}^z = \sum_l \hat{\sigma}_l^z$ . If we choose the energy eigenstates to be simultaneous eigenstates of  $\hat{S}^z$ , we have

$$\begin{aligned} \langle \alpha | \hat{\sigma}_l^z | \alpha \rangle &= \left( \langle \alpha | \hat{P}^x \right) \left( \hat{P}^x \hat{\sigma}_l^z \hat{P}^x \right) \left( \hat{P}^x | \alpha \rangle \right) \\ &= -\left( \langle \alpha | \hat{P}^x \right) \hat{\sigma}_l^z \left( \hat{P}^x | \alpha \rangle \right). \end{aligned} \quad (21)$$

Since  $\hat{P}^x$  and  $\hat{S}^z$  do not commute,  $\hat{P}^x | \alpha \rangle$  does not need to be  $e^{i\phi} | \alpha \rangle$ , so  $\langle \alpha | \hat{\sigma}_l^z | \alpha \rangle$  does not need to vanish. On the other hand, one can show that the matrix elements  $\langle \alpha | \hat{\sigma}_l^x | \alpha \rangle$  must vanish

$$\langle \alpha | \hat{\sigma}_l^x | \alpha \rangle = \langle \alpha | \hat{P}^z \left( \hat{P}^z \hat{\sigma}_l^x \hat{P}^z \right) \hat{P}^z | \alpha \rangle = -\langle \alpha | \hat{\sigma}_l^x | \alpha \rangle = 0. \quad (22)$$

(iii) The integrable Hamiltonian  $\hat{H}_I$  exhibits a supersymmetric point when [90, 91]

$$J^x J^y + J^x J^z + J^y J^z = 0. \quad (23)$$

Defining the operator  $\hat{P}_e^a = \prod_{l=1}^{L/2} \hat{\sigma}_{2l}^a$ , which acts only on even sites, we get  $\hat{P}_e^z \hat{H}_I(J^x, J^y, J^z) \hat{P}_e^z = \hat{H}_I(-J^x, -J^y, J^z)$ , and similarly for  $a = x, y$ . Hence, the supersymmetry also holds for

$$J^x J^y \pm J^x J^z \pm J^y J^z = 0. \quad (24)$$

Throughout this paper, we fix  $J^y = 1.0$  to be our energy scale,  $J^z = 1.5$ , and scan across  $J^x$ . For the integrable chain,  $\Lambda = 0$ , and for the nonintegrable one, we choose  $\Lambda = 0.2$ .

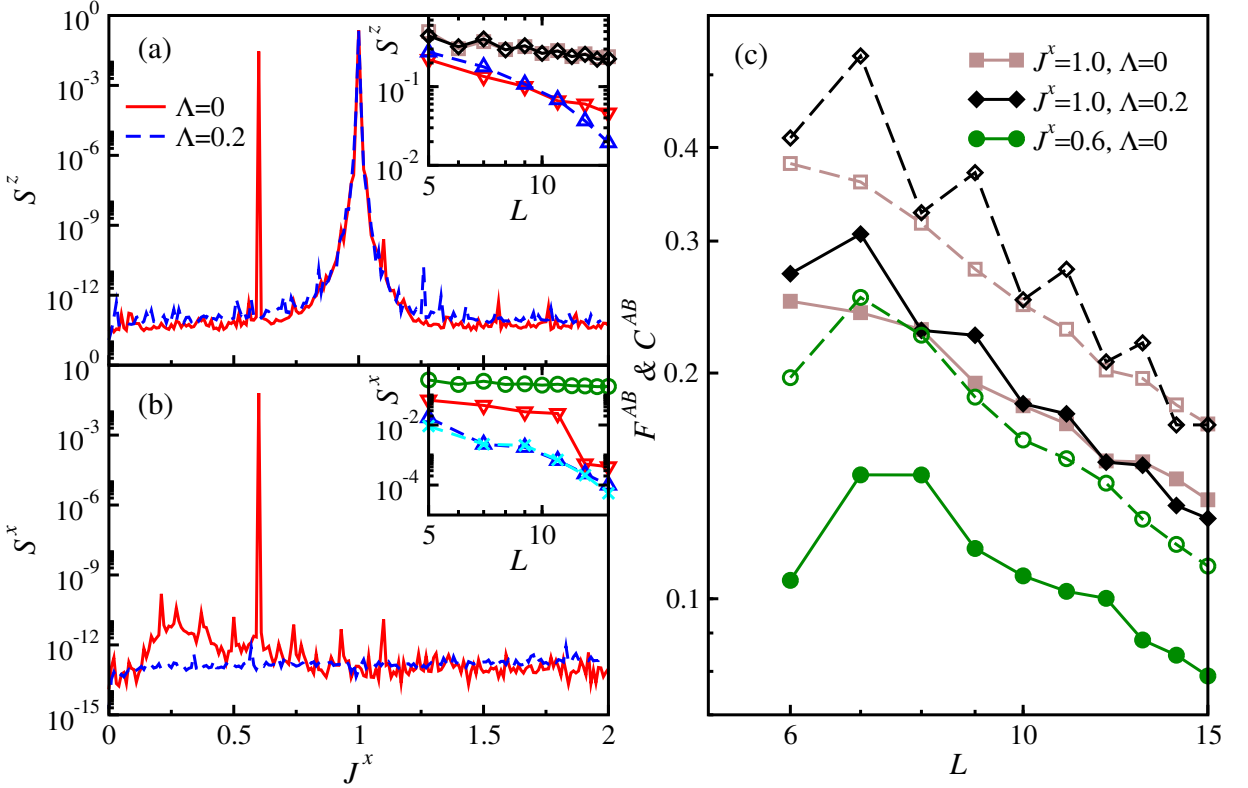


FIG. 1. Sum of the absolute values of the diagonal matrix elements of  $\hat{\sigma}_{L/2}^a$  in the energy eigenbasis. (a)  $S^z = \sum_{\alpha} |(\hat{\sigma}_{L/2}^z)_{\alpha\alpha}|$  and (b)  $S^x = \sum_{\alpha} |(\hat{\sigma}_{L/2}^x)_{\alpha\alpha}|$ , plotted as functions of the coupling parameter  $J^x$  for a chain with an even number of spins ( $L = 14$ ) for the integrable,  $\Lambda = 0$ , and non-integrable,  $\Lambda = 0.2$ , cases. Inset in (a), scaling of  $S^z$  as a function of  $L$  for  $J^x = 1.0, \Lambda = 0$  ( $\square$ ) and  $J^x = 1.0, \Lambda = 0.2$  ( $\diamond$ ); and (only showing results for odd values of  $L$ ) for  $J^x = 1.6, \Lambda = 0$  ( $\triangledown$ ) and  $J^x = 1.6, \Lambda = 0.2$  ( $\triangle$ ). Inset in (b), scaling of  $S^x$  as a function of  $L$  for  $J^x = 0.6, \Lambda = 0$  ( $\circ$ ); and (only showing results for odd values of  $L$ ) for  $J^x = 0.6, \Lambda = 0.2$  ( $\times$ ),  $J^x = 1.3, \Lambda = 0$  ( $\triangledown$ ), and  $J^x = 1.3, \Lambda = 0.2$  ( $\triangle$ ). (c) Infinite-time average  $F^{AB}(\infty)$  (solid lines with filled symbols) and  $C^{AB}(\infty)$  (dashed lines with empty symbols) as functions of  $L$  for  $\hat{A} = \hat{\sigma}_{L/2-1}^z$  and  $\hat{B} = \hat{\sigma}_{L/2+2}^z$  ( $\square$  for  $\Lambda = 0$  and  $\diamond$  for  $\Lambda = 0.2$ ) and for  $\hat{A} = \hat{\sigma}_{L/2-1}^x$  and  $\hat{B} = \hat{\sigma}_{L/2+2}^x$  ( $\circ$ ). In all panels, we show results for the XYZ chain with  $J^y = 1.0$  and  $J^z = 1.5$ .

### A. Relaxation dynamics and diagonal matrix elements of local operators

For the XYZ chain with an even number of sites, the diagonal matrix elements of  $\hat{\sigma}_l^a$  are large only when the system has additional symmetries, which can result in  $\hat{\sigma}_l^a$  overlapping with conserved quantities. This is illustrated in Fig. 1 (a) and Fig. 1 (b), where we plot the sum of the absolute values of the diagonal matrix elements of  $\hat{\sigma}_{L/2}^z$  and  $\hat{\sigma}_{L/2}^x$ , respectively, as functions of  $J^x$  for  $L = 14$ . They are denoted by

$$S^z = \sum_{\alpha} |(\hat{\sigma}_{L/2}^z)_{\alpha\alpha}|, \quad (25)$$

and

$$S^x = \sum_{\alpha} |(\hat{\sigma}_{L/2}^x)_{\alpha\alpha}|. \quad (26)$$

When  $J^x = 1$ , since  $J^x = J^y$ , the Hamiltonian has  $U(1)$  symmetry and conserves total magnetization in the  $z$ -

direction. For values of  $J^x$  close to 1 the total magnetization is a nearly-conserved quantity, which is known to result in prethermal behavior both in the integrable and nonintegrable cases [92]. This explains the “broad” peak of  $S^z$  at  $J^x = 1$  in Fig. 1(a) for both the integrable and the nonintegrable chains. The sharper peaks at  $J^x = 0.6$  for both  $S^z$  in Fig. 1(a) and  $S^x$  in Fig. 1(b) occur only in the integrable chain and are caused by the supersymmetric point satisfying Eq. (24).

For an odd number of sites, as mentioned before, the diagonal matrix elements of  $\hat{\sigma}_l^a$  need not vanish even if they vanish for an even number of sites. The inset in Fig. 1(a) [Fig. 1(b)] shows  $S^z$  [ $S^x$ ] as a function of  $L$  for  $J^x = 1, 1.6$  and  $\Lambda = 0, 0.2$  [ $J^x = 0.6, 1.3$  and  $\Lambda = 0, 0.2$ ]. For  $J^x = 1$  [inset of Fig. 1(a)] and  $J^x = 0.6$  with  $\Lambda = 0$  [inset of Fig. 1(b)], because of the presence of the  $U(1)$  symmetry and supersymmetry, respectively, both the  $L$  even and  $L$  odd systems have non-zero diagonal values. For the other parameters we only show results for  $L$  odd. In the latter cases we see that  $S^z$  and  $S^x$  decrease rapidly as  $L$  increases, i.e., the results for chains with  $L$

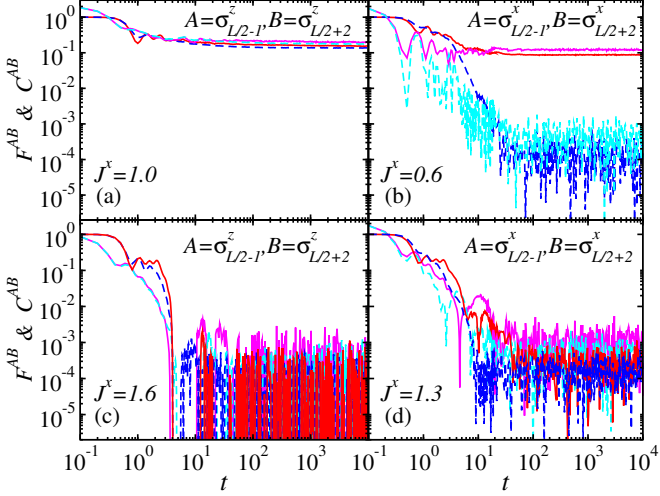


FIG. 2. Relaxation dynamics of  $F^{AB}(t)$  and  $C^{AB}(t)$  for the XYZ chain with  $J^y = 1.0$ ,  $J^z = 1.5$ , and  $L = 14$ . The solid lines correspond to the integrable model ( $\Lambda = 0$ ) and the dashed lines to the nonintegrable one ( $\Lambda = 0.2$ ). For the integrable (nonintegrable) model, the red (blue) line is for  $F^{AB}(t)$  and the pink (cyan) line for  $C^{AB}(t)$ .

odd approach the vanishing results for  $L$  even. Hence, we expect that Fig. 1(a) and Fig. 1(b) are representative of what happens in large chains no matter whether  $L$  is even or odd. See Appendix A for a comparison between the dynamics of OTOCs in systems with even and odd numbers of lattice sites.

For the three special sets of parameters for which large peaks are seen in Fig. 1(a), namely,  $J^x = 0.6$  and  $J^x = 1.0$  for the integrable model, and  $J^x = 1.0$ ,  $\Lambda = 0.2$  for the nonintegrable one, as well as in Fig. 1(b) for  $J^x = 0.6$  for the integrable model, the sum of the absolute values of the diagonal matrix elements decreases polynomially with  $L$ , as can be seen for  $S^z$  in the inset of Fig. 1(a) and for  $S^x$  in the inset of Fig. 1(b). This leads to the algebraic decay of the infinite-time averages of the OTOCs [two-time correlators] as functions of the system size, as predicted by Eq. (11) [Eq. (7)] and confirmed numerically in Fig. 1(c). In Fig. 1(c), we plot  $F^{\hat{\sigma}_{L/2-1}^z \hat{\sigma}_{L/2+2}^z}(\infty)$  [ $C^{\hat{\sigma}_{L/2-1}^z \hat{\sigma}_{L/2+2}^z}(\infty)$ ] for both the integrable and the nonintegrable chains with  $J^x = 1$ , and  $F^{\hat{\sigma}_{L/2-1}^x \hat{\sigma}_{L/2+2}^x}(\infty)$  [ $C^{\hat{\sigma}_{L/2-1}^x \hat{\sigma}_{L/2+2}^x}(\infty)$ ] for the integrable chain with  $J^x = 0.6$ . According to Eq. (12), we therefore expect that in the thermodynamic limit the OTOCs for these sets of parameters exhibit an algebraic decay.

In Fig. 2, we compare the dynamics of the OTOCs [ $F^{AB}(t)$ ] and of the two-time correlators [ $C^{AB}(t)$ ] for the integrable (solid lines) and nonintegrable (dashed lines) models. As expected from the analysis in Sec. II, we observe a remarkable qualitative (and quantitative in the cases of slow dynamics) resemblance in the relaxation dynamics of the OTOCs and the two-time correlators.

In Fig. 2(a) and Fig. 2(c),  $\hat{A} = \hat{\sigma}_{L/2-1}^z$  and  $\hat{B} = \hat{\sigma}_{L/2+2}^z$  for  $J^x = 1.0$  and  $J^x = 1.6$ , respectively. At the  $U(1)$

symmetric point,  $J^x = 1.0$ , considered in Fig. 2(a), the decay of the OTOC and of the two-time correlator are slow for the integrable and nonintegrable models, as expected. This contrasts with the fast relaxation seen for both models and quantities when we choose a value of  $J^x$  away from the peaks in Fig. 1(a) [ $J^x = 1.6$  in Fig. 2(c)], so that  $\hat{\sigma}_{L/2-1}^z$  and  $\hat{\sigma}_{L/2+2}^z$  have no diagonal matrix elements. The saturation and oscillations at long times in all panels of Fig. 2 are due to finite-size effects.

In Fig. 2(b) and Fig. 2(d), we show results for  $A = \hat{\sigma}_{L/2-1}^x$  and  $B = \hat{\sigma}_{L/2+2}^x$  for  $J^x = 0.6$  and  $J^x = 1.3$ , respectively. For the integrable case ( $\Lambda = 0$ ) at the supersymmetric point ( $J^x = 0.6$ ), Fig. 2(b) exhibits the expected slow decay of  $F^{AB}(t)$  and  $C^{AB}(t)$ . The behavior of both quantities for the nonintegrable case ( $\Lambda = 0.2$ ) in Fig. 2(b) resembles the dynamics of the supersymmetric model for short times ( $t \lesssim 2$ ), but the relaxation is fast for  $t \gtrsim 2$ . In Fig. 2(d), where  $J^x = 1.3$ , none of the models presents any special symmetry, so both the OTOC and the two-time correlator exhibit a fast (exponential-like) decay, similar to the one observed in Fig. 2(c).

## B. Relaxation dynamics and off-diagonal elements of local operators

The resemblance between the dynamics of the OTOC and the two-time correlator in the presence of symmetries seen in Sec. III A implies that the functions  $f^A(E_\infty, \omega)$  that characterize the off-diagonal matrix elements of  $\hat{\sigma}_i^a$  can be used to gain a qualitatively understanding of the OTOC decay in interacting integrable and nonintegrable many-body quantum models.  $f^A(E_\infty, \omega)$  is expected to exhibit different low-frequency behaviors depending on whether the OTOC decays slowly or fast.

Following the discussion in Sec. II B, we can match the relaxation dynamics of the OTOCs in Fig. 2 with the behavior of  $|f^A(E_\infty, \omega)|^2$  in Fig. 3. The smooth function  $|f^A(E_\infty, \omega)|^2$  is calculated from the variance  $\text{Var}$  of the off-diagonal matrix elements of  $A$  as  $|f^A(E_\infty, \omega)|^2 \approx \text{Var}(A_{\alpha\beta})$  [71, 84]. Specifically, we average over all off-diagonal matrix elements  $A_{\alpha\beta}$  in a frequency interval  $\Delta\omega = 0.01$  centered at points separated by  $\delta\omega = 0.002$ . In Fig. 3, we show results for three different system sizes, as indicated in the legend.

We find a one-to-one correspondence between Fig. 2 and Fig. 3. The OTOC decays slowly [Fig. 2(a) and Fig. 2(b) for the supersymmetric point] when  $|f^A(E_\infty, \omega)|^2$  exhibits a peak at low frequencies [Fig. 3(a) and Fig. 3(b) for the supersymmetric point], but it decays fast [Figs. 2(c) and 2(d), and Fig. 2(b) for the nonintegrable model] when  $|f^A(E_\infty, \omega)|^2$  exhibits a plateau at low frequencies [Figs. 3(c) and 3(d), and Fig. 3(b) for the nonintegrable model]. For the system sizes considered, one can see in Figs. 3(c) and 3(d) that  $|f^A(E_\infty, \omega)|^2$  is smoother at low frequencies for the nonintegrable model

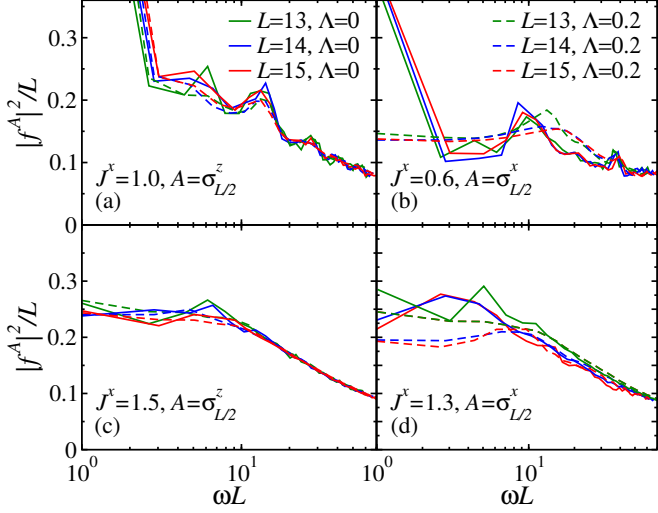


FIG. 3. Plots of  $|f^{\hat{\sigma}_L^z}(E_\infty, \omega)|^2 / L$  [(a) and (c)] and  $|f^{\hat{\sigma}_L^x}(E_\infty, \omega)|^2 / L$  [(b) and (d)] as functions of  $\omega L$  for the XYZ chain with  $J^y = 1.0$ ,  $J^z = 1.5$ , and  $L = 14$ . Solid (dashed) lines are for the integrable (nonintegrable) chain.

than for the integrable one. Since the results for the integrable model suffer from stronger finite-size effects, we expect those differences to disappear with increasing the system size.

#### IV. SUMMARY

The scrambling of quantum information as characterized by the relaxation dynamics of the OTOCs has been mainly investigated in nonintegrable models. Here, we extend these studies to interacting integrable models.

We show that the main factor determining the behavior of the OTOCs in interacting many-body quantum systems is the overlap between its constituent operators and conserved quantities of the model, rather than integrability or lack thereof. For the timescales explored in this work, if the overlap is large, the OTOCs decay slowly (algebraically-like) both for an integrable and a nonintegrable XYZ chain, while if the overlap is small the OTOCs decay rapidly (exponentially-like) for both the integrable and the nonintegrable finite XYZ chain.

Our numerical results can be understood, in a complementary manner, in terms of the behavior of the off-diagonal matrix elements of the OTOCs operators at low frequencies and of the scaling with the system size of the diagonal matrix elements.

Our analytical analysis, confirmed numerically, also indicates that in the presence of symmetries/local conserved quantities, the infinite-time average of the two-time correlators in finite systems determines the infinite-

time average of the OTOC. Hence, a slow relaxation of one of the two-time correlators implies a slow relaxation of the OTOC. The slow relaxation dynamics stems from the slow evolution (in the space of Pauli strings) of the individual operators, which in turn is due to the presence of symmetries.

#### ACKNOWLEDGMENTS

L.F.S. is supported by the United States National Science Foundation (NSF) Grant No. DMR-1936006 and the MPS Simons Foundation Award ID: 678586. M.R. is supported by the United States National Science Foundation (NSF) Grant No. PHY-2012145. D.P. acknowledges support from the Ministry of Education Singapore, under the grant MOE-T2EP50120-0019. The computational work for this article were partially performed on the National Supercomputing Centre, Singapore [93].

#### Appendix A: Even vs odd chains

A comparison between the decay of the OTOCs for even and odd chains without conservation laws is provided in Fig. 4 for the integrable [Fig. 4(a), Fig. 4(b)] and the nonintegrable [Fig. 4(c), Fig. 4(d)] model. As the system size increases, one can see an increase of the time up to which the dynamics for the even and odd sizes coincide. This lends support to our conclusion that for sufficiently large system sizes our analysis based only on the study of even system sizes will also apply to odd system sizes.

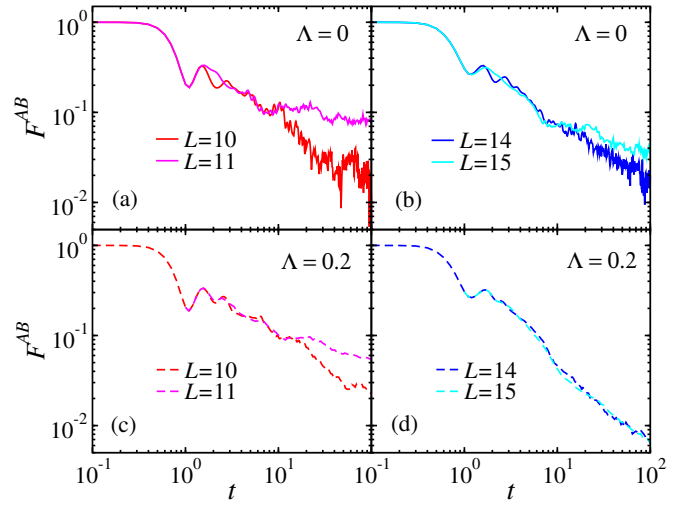


FIG. 4. Comparison of the relaxation dynamics of  $F^{\hat{\sigma}_{L/2-1}^z \hat{\sigma}_{L/2+2}^z}$  for different sizes of the XYZ chain with  $J^x = 0.8$ ,  $J^y = 1.0$ , and  $J^z = 1.5$ . Solid (dashed) lines are for the integrable (nonintegrable) chain.

---

[1] E. Witten, Anti-de Sitter space and holography, *Adv. Theor. Math. Phys.* **2**, 253 (1998), arXiv:hep-th/9802150.

[2] J. Maldacena, *Int. J. Theor. Phys.* **38**, 1113–1133 (1999).

[3] P. Hayden and J. Preskill, Black holes as mirrors: quantum information in random subsystems, *J. High Energy Phys.* **2007** (09), 120–120.

[4] Y. Sekino and L. Susskind, Fast scramblers, *J. High Energy Phys.* **2008** (10), 065–065.

[5] S. H. Shenker and D. Stanford, Black holes and the butterfly effect, *J. High Energy Phys.* **2014** (3).

[6] S. Sachdev and J. Ye, Gapless spin-fluid ground state in a random quantum Heisenberg magnet, *Phys. Rev. Lett.* **70**, 3339 (1993).

[7] A. Kitaev, A simple model of quantum holography, *Talks at KITP* (2015).

[8] N. Lashkari, D. Stanford, M. Hastings, T. Osborne, and P. Hayden, Towards the fast scrambling conjecture, *J. High Energy Phys.* **2013** (4).

[9] D. A. Roberts and D. Stanford, Diagnosing chaos using four-point functions in two-dimensional conformal field theory, *Phys. Rev. Lett.* **115**, 131603 (2015).

[10] J. S. Cotler, G. Gur-Ari, M. Hanada, J. Polchinski, P. Saad, S. H. Shenker, D. Stanford, A. Streicher, and M. Tezuka, Black holes and random matrices, *J. High Energy Phys.* **2017** (5).

[11] D. A. Roberts, D. Stanford, and L. Susskind, Localized shocks, *J. High Energy Phys.* **2015** (3).

[12] P. Hosur, X.-L. Qi, D. A. Roberts, and B. Yoshida, Chaos in quantum channels, *J. High Energy Phys.* **2016** (2).

[13] F. Borgonovi, F. M. Izrailev, and L. F. Santos, Timescales in the quench dynamics of many-body quantum systems: Participation ratio versus out-of-time ordered correlator, *Phys. Rev. E* **99**, 052143 (2019).

[14] I. García-Mata, R. A. Jalabert, and D. A. Wisniacki, Out-of-time-order correlators and quantum chaos (2022), 2209.07965.

[15] J. Li, R. Fan, H. Wang, B. Ye, B. Zeng, H. Zhai, X. Peng, and J. Du, Measuring out-of-time-order correlators on a nuclear magnetic resonance quantum simulator, *Phys. Rev. X* **7**, 031011 (2017).

[16] M. Gärttner, J. G. Bohnet, A. Safavi-Naini, M. L. Wall, J. J. Bollinger, and A. M. Rey, Measuring out-of-time-order correlations and multiple quantum spectra in a trapped-ion quantum magnet, *Nat. Phys.* **13**, 781–786 (2017).

[17] K. X. Wei, C. Ramanathan, and P. Cappellaro, Exploring localization in nuclear spin chains, *Phys. Rev. Lett.* **120**, 070501 (2018).

[18] K. A. Landsman, C. Figgatt, T. Schuster, N. M. Linke, B. Yoshida, N. Y. Yao, and C. Monroe, Verified quantum information scrambling, *Nature* **567**, 61–65 (2019).

[19] M. Niknam, L. F. Santos, and D. G. Cory, Sensitivity of quantum information to environment perturbations measured with a nonlocal out-of-time-order correlation function, *Phys. Rev. Research* **2**, 013200 (2020).

[20] M. K. Joshi, A. Elben, B. Vermersch, T. Brydges, C. Maier, P. Zoller, R. Blatt, and C. F. Roos, Quantum information scrambling in a trapped-ion quantum simulator with tunable range interactions, *Phys. Rev. Lett.* **124**, 240505 (2020).

[21] M. S. Blok, V. V. Ramasesh, T. Schuster, K. O'Brien, J. M. Kreikebaum, D. Dahlen, A. Morvan, B. Yoshida, N. Y. Yao, and I. Siddiqi, Quantum information scrambling on a superconducting qutrit processor, *Phys. Rev. X* **11**, 021010 (2021).

[22] X. Mi, P. Roushan, C. Quintana, S. Mandra, J. Marshall, C. Neill, F. Arute, K. Arya, J. Atalaya, R. Babbush, J. C. Bardin, R. Barends, A. Bengtsson, S. Boixo, A. Bouassa, M. Broughton, B. B. Buckley, D. A. Buell, B. Burkett, N. Bushnell, Z. Chen, B. Chiaro, R. Collins, W. Courtney, S. Demura, A. R. Derk, A. Dunsworth, D. Eppens, C. Erickson, E. Farhi, A. G. Fowler, B. Foxen, C. Gidney, M. Giustina, J. A. Gross, M. P. Harrigan, S. D. Harrington, J. Hilton, A. Ho, S. Hong, T. Huang, W. J. Huggins, L. B. Ioffe, S. V. Isakov, E. Jeffrey, Z. Jiang, C. Jones, D. Kafri, J. Kelly, S. Kim, A. Kitaev, P. V. Klimov, A. N. Korotkov, F. Kostritsa, D. Landhuis, P. Laptev, E. Lucero, O. Martin, J. R. McClean, T. McCourt, M. McEwen, A. Megrant, K. C. Miao, M. Mohseni, W. Mruczkiewicz, J. Mutus, O. Naaman, M. Neeley, M. Newman, M. Y. Niu, T. E. O'Brien, A. Opremcak, E. Ostby, B. Pato, A. Petukhov, N. Redd, N. C. Rubin, D. Sank, K. J. Satzinger, V. Shvarts, D. Strain, M. Szalay, M. D. Trevithick, B. Villalonga, T. White, Z. J. Yao, P. Yeh, A. Zalcman, H. Neven, I. Aleiner, K. Kechedzhi, V. Smelyanskiy, and Y. Chen, Information scrambling in computationally complex quantum circuits (2021), arXiv:2101.08870 [quant-ph].

[23] J. Braumüller, A. H. Karamlou, Y. Yanay, B. Kannan, D. Kim, M. Kjaergaard, A. Melville, B. M. Niedzielski, Y. Sung, A. Vepsäläinen, R. Winik, J. L. Yoder, T. P. Orlando, S. Gustavsson, C. Tahan, and W. D. Oliver, Probing quantum information propagation with out-of-time-ordered correlators (2021), arXiv:2102.11751 [quant-ph].

[24] E. B. Rozenbaum, S. Ganeshan, and V. Galitski, Lyapunov exponent and out-of-time-ordered correlator's growth rate in a chaotic system, *Phys. Rev. Lett.* **118**, 086801 (2017).

[25] K. Hashimoto, K. Murata, and R. Yoshii, Out-of-time-order correlators in quantum mechanics, *J. High Energy Phys.* **2017** (10).

[26] J. S. Cotler, D. Ding, and G. R. Penington, Out-of-time-order operators and the butterfly effect, *Ann. Phys.* **396**, 318–333 (2018).

[27] I. García-Mata, M. Saraceno, R. A. Jalabert, A. J. Roncaglia, and D. A. Wisniacki, Chaos signatures in the short and long time behavior of the out-of-time ordered correlator, *Phys. Rev. Lett.* **121**, 210601 (2018).

[28] S. Ray, S. Sinha, and K. Sengupta, Signature of chaos and delocalization in a periodically driven many-body system: An out-of-time-order-correlation study, *Phys. Rev. A* **98**, 053631 (2018).

[29] J. Chávez-Carlos, B. López-del Carpio, M. A. Bastarrachea-Magnani, P. Stránský, S. Lerma-Hernández, L. F. Santos, and J. G. Hirsch, Quantum and classical Lyapunov exponents in atom-field interaction systems, *Phys. Rev. Lett.* **122**, 024101 (2019).

[30] E. M. Fortes, I. García-Mata, R. A. Jalabert, and D. A. Wisniacki, Gauging classical and quantum integrability through out-of-time-ordered correlators, *Phys. Rev. E* **100**, 042201 (2019).

[31] J. Rammensee, J. D. Urbina, and K. Richter, Many-body quantum interference and the saturation of out-of-time-order correlators, *Phys. Rev. Lett.* **121**, 124101 (2018).

[32] R. Prakash and A. Lakshminarayan, Scrambling in strongly chaotic weakly coupled bipartite systems: Universality beyond the ehrenfest timescale, *Phys. Rev. B* **101**, 121108(R) (2020).

[33] P. D. Bergamasco, G. G. Carlo, and A. M. F. Rivas, Out-of-time ordered correlators, complexity, and entropy in bipartite systems, *Phys. Rev. Research* **1**, 033044 (2019).

[34] E. B. Rozenbaum, L. A. Bunimovich, and V. Galitski, Early-time exponential instabilities in nonchaotic quantum systems, *Phys. Rev. Lett.* **125**, 014101 (2020).

[35] J. Wang, G. Benenti, G. Casati, and W.-g. Wang, Complexity of quantum motion and quantum-classical correspondence: A phase-space approach, *Phys. Rev. Research* **2**, 043178 (2020).

[36] J. Wang, G. Benenti, G. Casati, and W.-g. Wang, Quantum chaos and the correspondence principle, *Phys. Rev. E* **103**, L030201 (2021).

[37] S. Pappalardi, A. Russomanno, B. Žunkovič, F. Iemini, A. Silva, and R. Fazio, Scrambling and entanglement spreading in long-range spin chains, *Phys. Rev. B* **98**, 134303 (2018).

[38] Q. Hummel, B. Geiger, J. D. Urbina, and K. Richter, Reversible quantum information spreading in many-body systems near criticality, *Phys. Rev. Lett.* **123**, 160401 (2019).

[39] S. Pilatowsky-Cameo, J. Chávez-Carlos, M. A. Bastarrachea-Magnani, P. Stránský, S. Lerma-Hernández, L. F. Santos, and J. G. Hirsch, Positive quantum Lyapunov exponents in experimental systems with a regular classical limit, *Phys. Rev. E* **101**, 010202(R) (2020).

[40] T. Xu, T. Scaffidi, and X. Cao, Does scrambling equal chaos?, *Phys. Rev. Lett.* **124**, 140602 (2020).

[41] K. Hashimoto, K.-B. Huh, K.-Y. Kim, and R. Watanabe, Exponential growth of out-of-time-order correlator without chaos: inverted harmonic oscillator, *J. High En. Phys.* **2020**, 68 (2020).

[42] J. Chavez-Carlos, T. L. M. Lezama, R. G. Cortinas, J. Venkatraman, M. H. Devoret, V. S. Batista, F. Perez-Bernal, and L. F. Santos, Spectral kissing and its dynamical consequences in the squeezed Kerr-nonlinear oscillator (2022), arXiv:2210.07255.

[43] T. Rakovszky, F. Pollmann, and C. W. von Keyserlingk, Diffusive hydrodynamics of out-of-time-ordered correlators with charge conservation, *Phys. Rev. X* **8**, 031058 (2018).

[44] A. Nahum, J. Ruhman, S. Vijay, and J. Haah, Quantum entanglement growth under random unitary dynamics, *Phys. Rev. X* **7**, 031016 (2017).

[45] A. Nahum, S. Vijay, and J. Haah, Operator spreading in random unitary circuits, *Phys. Rev. X* **8**, 021014 (2018).

[46] C. W. von Keyserlingk, T. Rakovszky, F. Pollmann, and S. L. Sondhi, Operator hydrodynamics, otocs, and entanglement growth in systems without conservation laws, *Phys. Rev. X* **8**, 021013 (2018).

[47] V. Khemani, A. Vishwanath, and D. A. Huse, Operator spreading and the emergence of dissipative hydrodynamics under unitary evolution with conservation laws, *Phys. Rev. X* **8**, 031057 (2018).

[48] V. Balachandran, G. Benenti, G. Casati, and D. Polletti, From the eigenstate thermalization hypothesis to algebraic relaxation of OTOCs in systems with conserved quantities, *Phys. Rev. B* **104**, 10.1103/physrevb.104.104306 (2021).

[49] D. J. Luitz and Y. Bar Lev, Information propagation in isolated quantum systems, *Phys. Rev. B* **96**, 020406 (2017).

[50] L. Colmenarez and D. J. Luitz, Lieb-robinson bounds and out-of-time order correlators in a long-range spin chain, *Phys. Rev. Research* **2**, 043047 (2020).

[51] I. Bloch, J. Dalibard, and W. Zwerger, Many-body physics with ultracold gases, *Rev. Mod. Phys.* **80**, 885 (2008).

[52] M. A. Cazalilla, R. Citro, T. Giamarchi, E. Orignac, and M. Rigol, One dimensional bosons: From condensed matter systems to ultracold gases, *Rev. Mod. Phys.* **83**, 1405 (2011).

[53] P. Calabrese, F. H. L. Essler, and G. Mussardo, Introduction to ‘quantum integrability in out of equilibrium systems’, *J. Stat. Mech.* **2016**, 064001 (2016).

[54] T. Kinoshita, T. Wenger, and D. S. Weiss, A quantum Newton’s cradle, *Nature* **440**, 900 (2006).

[55] T. Langen, S. Erne, R. Geiger, B. Rauer, T. Schweigler, M. Kuhnert, W. Rohringer, I. E. Mazets, T. Gasenzer, and J. Schmiedmayer, Experimental observation of a generalized Gibbs ensemble, *Science* **348**, 207 (2015).

[56] Y. Tang, W. Kao, K.-Y. Li, S. Seo, K. Mallayya, M. Rigol, S. Gopalakrishnan, and B. L. Lev, Thermalization near integrability in a dipolar quantum Newton’s cradle, *Phys. Rev. X* **8**, 021030 (2018).

[57] M. Rigol, V. Dunjko, V. Yurovsky, and M. Olshanii, Relaxation in a completely integrable many-body quantum system: An ab initio study of the dynamics of the highly excited states of 1d lattice hard-core bosons, *Phys. Rev. Lett.* **98**, 050405 (2007).

[58] E. Ilievski, J. De Nardis, B. Wouters, J.-S. Caux, F. H. L. Essler, and T. Prosen, Complete generalized Gibbs ensembles in an interacting theory, *Phys. Rev. Lett.* **115**, 157201 (2015).

[59] L. Vidmar and M. Rigol, Generalized Gibbs ensemble in integrable lattice models, *J. Stat. Mech.* **2016**, 064007 (2016).

[60] M. Schemmer, I. Bouchoule, B. Doyon, and J. Dubail, Generalized hydrodynamics on an atom chip, *Phys. Rev. Lett.* **122**, 090601 (2019).

[61] J. M. Wilson, N. Malvania, Y. Le, Y. Zhang, M. Rigol, and D. S. Weiss, Observation of dynamical fermionization, *Science* **367**, 1461 (2020).

[62] N. Malvania, Y. Zhang, Y. Le, J. Dubail, M. Rigol, and D. S. Weiss, Generalized hydrodynamics in strongly interacting 1D Bose gases, *Science* **373**, 1129 (2021).

[63] O. A. Castro-Alvaredo, B. Doyon, and T. Yoshimura, Emergent hydrodynamics in integrable quantum systems out of equilibrium, *Phys. Rev. X* **6**, 041065 (2016).

[64] B. Bertini, M. Collura, J. De Nardis, and M. Fagotti, Transport in out-of-equilibrium XXZ chains: Exact profiles of charges and currents, *Phys. Rev. Lett.* **117**, 207201 (2016).

[65] M. Srednicki, The approach to thermal equilibrium in quantized chaotic systems, *J. Phys. A* **32**, 1163 (1999).

[66] Y. Huang, F. G. S. L. Brandão, and Y.-L. Zhang, Finite-size scaling of out-of-time-ordered correlators at late times, *Phys. Rev. Lett.* **123**, 010601 (2019).

[67] P. R. Zangara, A. D. Dente, E. J. Torres-Herrera, H. M. Pastawski, A. Iucci, and L. F. Santos, Time fluctua-

tions in isolated quantum systems of interacting particles, *Phys. Rev. E* **88**, 032913 (2013).

[68] L. D’Alessio, Y. Kafri, A. Polkovnikov, and M. Rigol, From quantum chaos and eigenstate thermalization to statistical mechanics and thermodynamics, *Adv. Phys.* **65**, 239–362 (2016).

[69] H. Kim, T. N. Ikeda, and D. A. Huse, Testing whether all eigenstates obey the eigenstate thermalization hypothesis, *Phys. Rev. E* **90**, 052105 (2014).

[70] R. Mondaini, K. R. Fratus, M. Srednicki, and M. Rigol, Eigenstate thermalization in the two-dimensional transverse field ising model, *Phys. Rev. E* **93**, 032104 (2016).

[71] T. LeBlond, K. Mallayya, L. Vidmar, and M. Rigol, Entanglement and matrix elements of observables in interacting integrable systems, *Phys. Rev. E* **100**, 062134 (2019).

[72] G. Biroli, C. Kollath, and A. M. Läuchli, Effect of rare fluctuations on the thermalization of isolated quantum systems, *Phys. Rev. Lett.* **105**, 250401 (2010).

[73] T. N. Ikeda, Y. Watanabe, and M. Ueda, Finite-size scaling analysis of the eigenstate thermalization hypothesis in a one-dimensional interacting bose gas, *Phys. Rev. E* **87**, 012125 (2013).

[74] W. Beugeling, R. Moessner, and M. Haque, Finite-size scaling of eigenstate thermalization, *Phys. Rev. E* **89**, 042112 (2014).

[75] V. Alba, Eigenstate thermalization hypothesis and integrability in quantum spin chains, *Phys. Rev. B* **91**, 155123 (2015).

[76] Y. Zhang, L. Vidmar, and M. Rigol, Statistical properties of the off-diagonal matrix elements of observables in eigenstates of integrable systems, arXiv:2203.06294.

[77] E. H. Lieb and D. W. Robinson, The finite group velocity of quantum spin systems, *Comm. Math. Phys.* **28**, 251 (1972).

[78] M. Cheneau, P. Barmettler, D. Poletti, M. Endres, P. Schauß, T. Fukuhara, C. Gross, I. Bloch, C. Kollath, and S. Kuhr, Light-cone-like spreading of correlations in a quantum many-body system, *Nature* **481**, 484 (2012).

[79] D. J. Luitz, R. Moessner, S. L. Sondhi, and V. Khemani, Prethermalization without temperature, *Phys. Rev. X* **10**, 021046 (2020).

[80] J. Lee, D. Kim, and D.-H. Kim, Typical growth behavior of the out-of-time-ordered commutator in many-body localized systems, *Phys. Rev. B* **99**, 184202 (2019).

[81] J. M. Deutsch, Quantum statistical mechanics in a closed system, *Phys. Rev. A* **43**, 2046 (1991).

[82] M. Srednicki, Chaos and quantum thermalization, *Phys. Rev. E* **50**, 888 (1994).

[83] M. Rigol, V. Dunjko, and M. Olshanii, Thermalization and its mechanism for generic isolated quantum systems, *Nature* **452**, 854–858 (2008).

[84] T. LeBlond and M. Rigol, Eigenstate thermalization for observables that break hamiltonian symmetries and its counterpart in interacting integrable systems, *Phys. Rev. E* **102**, 062113 (2020).

[85] M. Brenes, T. LeBlond, J. Goold, and M. Rigol, Eigenstate thermalization in a locally perturbed integrable system, *Phys. Rev. Lett.* **125**, 070605 (2020).

[86] M. Brenes, J. Goold, and M. Rigol, Low-frequency behavior of off-diagonal matrix elements in the integrable XXZ chain and in a locally perturbed quantum-chaotic XXZ chain, *Phys. Rev. B* **102**, 075127 (2020).

[87] R. J. Baxter, Eight-vertex model in lattice statistics, *Phys. Rev. Lett.* **26**, 832 (1971).

[88] R. J. Baxter, Partition function of the eight-vertex lattice model, *Ann. Phys.* **70**, 193 (1972).

[89] S. M. Giampaolo, F. B. Ramos, and F. Franchini, The frustration of being odd: universal area law violation in local systems, *J. Phys. Comm.* **3**, 081001 (2019).

[90] C. Hagendorf and P. Fendley, The eight-vertex model and lattice supersymmetry, *J. Stat. Phys.* **146**, 1122 (2012).

[91] J. Liénardy, Integrable lattice models and supersymmetry, Ph.D. thesis (2020).

[92] K. Mallayya, M. Rigol, and W. De Roeck, Prethermalization and thermalization in isolated quantum systems, *Phys. Rev. X* **9**, 021027 (2019).

[93] <https://www.nscc.sg/>.